A Numerical Study on Régime Transitions of the Rotating Annulus Flow with a Semi-Spectral Model

By Seiji Sugata[1] and Shigeo Yoden

Department of Geophysics, Kyoto University, Kyoto 606-01, Japan
(Manuscript received 29 January 1993, in revised form 7 June 1993)

Abstract

Some of the rotating annulus experiments with radial differential heating show stepwise transitions of flow régimes from steady axi-symmetric flow to vacillation via a steady wave régime as the rotation rate increases. The stepwise régime transitions are investigated numerically with a semi-spectral model of a three-dimensional Boussinesq fluid, and the results are interpreted with bifurcation theories. The transition between axi-symmetric flow and a steady wave régime is characterized by hysteresis; the criterion for the disappearance of an established steady wave differs from the criterion for the onset of the steady wave. The branch of the steady wave solution does not bifurcate from that of the axi-symmetric flow at the point where the axi-symmetric flow becomes unstable. Instead, the steady wave branch has another type of critical point (interpreted as a "limit point") at which it disappears. The transition from steady wave to tilted-trough vacillation is interpreted as a Hopf bifurcation; a periodically fluctuating solution bifurcates from the steady wave branch when the steady wave solution loses its stability.

1. Introduction

Hydrodynamic instabilities and the corresponding transitions of flow régimes have been one of the interesting subjects in contemporary fluid dynamics (*e.g.* Swinney and Gollub, 1981). When an experimental parameter is changed gradually, stepwise transitions from a steady symmetric flow to irregular turbulent flow are observed in some experiments such as the Rayleigh-Bénard convection and the Taylor-Couette flow. Modern technology in laboratory experiments and advanced computing facilities for numerical experiments have improved our understanding of the transitions of flow régimes. Moreover, bifurcation theories and chaos theories have given fundamental concepts of the transitions of flow régimes.

Some of the rotating annulus experiments with radial differential heating, which contain the basic dynamics of the general circulation of the atmosphere, show similar stepwise transitions from steady axi-symmetric flow to irregular turbulent flow via steady wave and vacillation régimes (see *e.g.* Hide and Mason, 1975). A régime diagram obtained by Fowlis and Hide (1965) is shown in Fig. 1 together with recent results by Tamaki and Ukaji (1985; hereafter referred to as TU85) and Ukaji and Tamaki (1989, 1990; hereafter UT89 and UT90, respectively). The flow régimes are mainly dependent on two non-dimensional parameters of the Taylor number, Ta (the abscissa) and the thermal Rossby number, Ro_T (the ordinate). If the rotation rate Ω of the annulus is increased gradually with a constant temperature difference ΔT between the outer and inner walls, say $\Delta T = 3\,\mathrm{K}$ indicated by a straight line in Fig. 1, a sequence of régime transitions are obtained from steady axi-symmetric flow to irregular flow. In some laboratory experiments (*e.g.* Fultz *et al.*, 1959; TU85; Hignett, 1985), hysteresis is observed at the transition from the axi-symmetric to wave régime and in the wave régime; two or more stable states may exist for the same experimental parameters depending on the initial conditions. In addition, a new class of amplitude vacillations, which are adjacent to a transition to the next lowest wavenumber as shown in Fig. 1 with $\Delta T = 8\,\mathrm{K}$, are also obtained by TU85 and by Hignett (1985).

The transition from axi-symmetric flow to a wave régime was firstly investigated by Lorenz (1962) with a low-order model of a two-layer quasi-geostrophic fluid system. He analyzed a set of nonlinear ordinary differential equations with 8 dependent variables obtained by means of highly truncated Fourier-Bessel series. He proved with the simplified model that the steady axi-symmetric flow is always possible in a mathematical sense but unsta-

[1]Present affiliation: The National Institute for Environmental Studies, Tsukuba, Ibaraki 305, Japan.

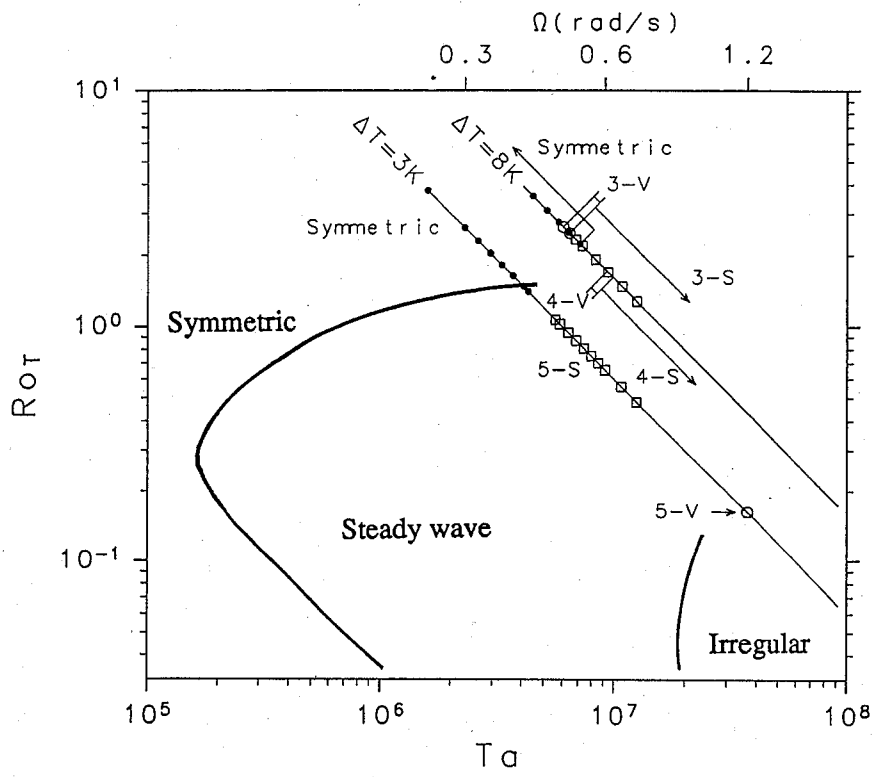

Fig. 1. Régime diagram obtained by Fowlis and Hide (1965), together with the results by Tamaki and Ukaji (1985) and Ukaji and Tamaki (1989, 1990) along two diagonal lines of constant temperature difference $\Delta T = 3$ K and 8 K. Dots denote axi-symmetric flow, m-S a steady wave of the dominant wavenumber m, and m-V vacillation of the dominant wavenumber m.

ble with respect to wave disturbance for certain combinations of Ta and Ro_T, that is, the inside of an anvil-shaped curve in the régime diagram. The transition occurs as a manifestation of baroclinic instability of the axi-symmetric flow. Moreover, hysteresis in the upper transition for large Ta is obtained in his low-order model in agreement with the laboratory experiments by Fultz *et al.* (1959): the criterion for the disappearance of an established steady wave differs from the criterion for the onset of the steady wave. Matsuda and Yoden (1985) illustrated a bifurcation diagram for the hysteresis based on these results.

Lorenz (1963) modified the model to explore further transitions of régimes. The geometry of the cylindrical annulus was changed to an infinite channel with a double-Fourier series and the second lateral mode was retained to get a non-linear system of 14 variables. Numerical solutions of vacillations and irregular flows were obtained by time integrations, in addition to analytic solutions of axi-symmetric flows and steady waves. Extension of this Lorenz model was done by Quinet (1973a, b) and Yoden (1979) with the inclusion of some higher modes to investigate the structure of non-linear processes in the flow régime transitions further. Detailed analysis of the régime transitions in the Lorenz model was done by Ghil and Childress (1987) with bifurcation theory. Figure 2 is a bifurcation diagram showing the dependence of solutions on the external parameter k^{-1} that is regarded as a rotation rate. As k^{-1} is increased in the diagram, the axi-symmetric flow (denoted by H) loses its stability at the point A and a steady wave solution of the first mode (R_1) bifurcates from the point. At the point B the wave solution R_1 becomes unstable and two steady-wave branches of R'_{12} and R''_{12} bifurcate. Solutions R'_{12} and R''_{12} differ from each other only in the sign of the second lateral mode, owing to the spatial symmetry of the mode (Yoden, 1985). A Hopf bifurcation takes place at D′ (D″) and a stable periodic solution UV' (UV'') appears, which is a class of tilted-trough vacillation. Finally, non-periodic chaotic solutions (T) appear after some further bifurcations. The sequence of bifurcations leads to solutions of increasing spatial and temporal complexity, as the simpler solutions lose their stability. A general theory of the symmetry-breaking in spatial structures at bifurcation points was given by Matsuda (1983).

Stepwise transitions from steady axi-symmetric flow to irregular turbulent flow with increasing complexity of flow patterns are *qualitatively* illustrated in the Lorenz model. Detailed analysis of the model is possible because its dependent variables

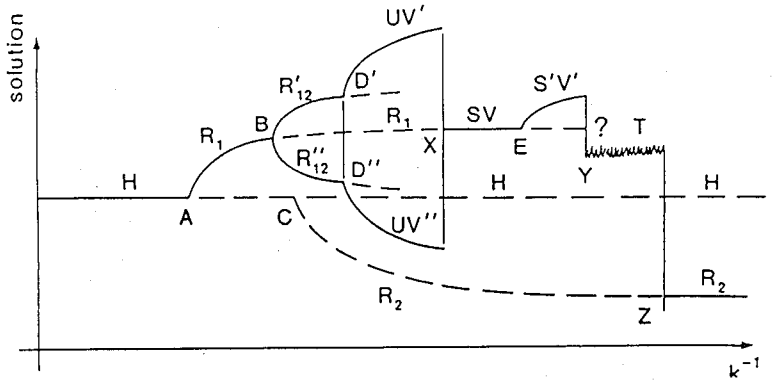

Fig. 2. Bifurcation diagram for the Lorenz (1963) model drawn by Ghil and Childress (1987). The solid line is a branch of the stable solution, the dashed line that of an unstable one. The abscissa is a bifurcation parameter proportional to the rotation rate. See text for details.

are of the order of O (10) owing to the severe truncation. However, several crude assumptions (approximations) were also made to obtain the model: quasi-geostrophy, a two-layer system, Ekman friction, non-existence of lateral boundary layers, and so on.

A quite different approach in numerical studies on the rotating annulus flows originated from Williams (1967a, 1967b, 1969). He solved two- or three-dimensional Navier-Stokes equations numerically without many approximations. Advances in computing facilities over these years have made it possible to compare numerical simulations directly with laboratory measurements (*e.g.* Hignett *et al.*, 1985; UT89; UT90; Sugata and Yoden, 1991). Recently, Miller and Butler (1991) investigated the hysteresis in the transition between axi-symmetric flow and the steady wave régime with a semi-spectral model of Boussinesq fluid. They obtained the hysteresis for large ΔT only in the case of a free surface, which result was consistent with the laboratory experiment by Fein (1973). The spatial structure of the flow field and energetics in the hysteresis were also diagnosed carefully with the three-dimensional data obtained. Investigation of further transitions of flow régimes was left for future study.

In this study, we develop a similar semi-spectral model without many approximations to investigate the stepwise transitions of flow régimes in the rotating annulus experiments. The transition to tilted-trough vacillation is clarified as well as the transition between axi-symmetric flow and steady wave régime. Our model is similar to that introduced by Miller and Butler (1991) but includes wave-wave interactions with the first harmonics. However, the present semi-spectral model has limitations for the study of some vacillations in which side-bands of the dominant wave may play an important rôle (*e.g.* Pfeffer *et al.*, 1980). Numerical results are interpreted with bifurcation theories.

2. The model

We consider water contained between two coaxial cylinders of inner and outer radii a and b, respectively, and two parallel horizontal planes of depth H. The dimensions are $a=4.5$ cm, $b=9.7$ cm and $H=8.0$ cm, which are the same as those in TU85, UT89 and UT90. The top surface is assumed to be a free-slip surface at $z=H$ with no undulation. The other three bonding surfaces are rigid. The inner and outer walls are held at different constant temperatures, T_a and T_b ($T_a<T_b$), to maintain the difference ΔT. The top and bottom boundaries are thermally insulating. The container rotates at a constant rate Ω. Controllable experimental parameters are ΔT and Ω.

The governing equations under the Boussinesq approximation are:

$$u_t + uu_r + \frac{vu_\lambda}{r} + wu_z - \frac{v^2}{r} - 2\Omega v = -p_r + \nu\left[u_{zz} + \frac{1}{r^2}u_{\lambda\lambda} - w_{rz} - \frac{1}{r^2}(rv_\lambda)_r\right], \tag{1}$$

$$v_t + uv_r + \frac{vv_\lambda}{r} + wv_z + \frac{uv}{r} + 2\Omega u = -\frac{p_\lambda}{r} + \nu\left[\left\{\frac{1}{r}(rv)_r\right\}_r + v_{zz} - \left(\frac{u}{r}\right)_{r\lambda} - \frac{1}{r}w_{z\lambda}\right], \tag{2}$$

$$w_t + uw_r + \frac{vw_\lambda}{r} + ww_z = -p_z + \nu\left[\frac{1}{r}(rw_r)_r + \frac{1}{r^2}w_{\lambda\lambda} - \frac{1}{r}v_{z\lambda} - \frac{1}{r}(ru_z)_r\right] + \alpha\Delta T\theta g, \tag{3}$$

$$\theta_t + u\theta_r + \frac{v\theta_\lambda}{r} + w\theta_z = \kappa\left[\theta_{rr} + \frac{1}{r}\theta_r + \frac{1}{r^2}\theta_{\lambda\lambda} + \theta_{zz}\right], \tag{4}$$

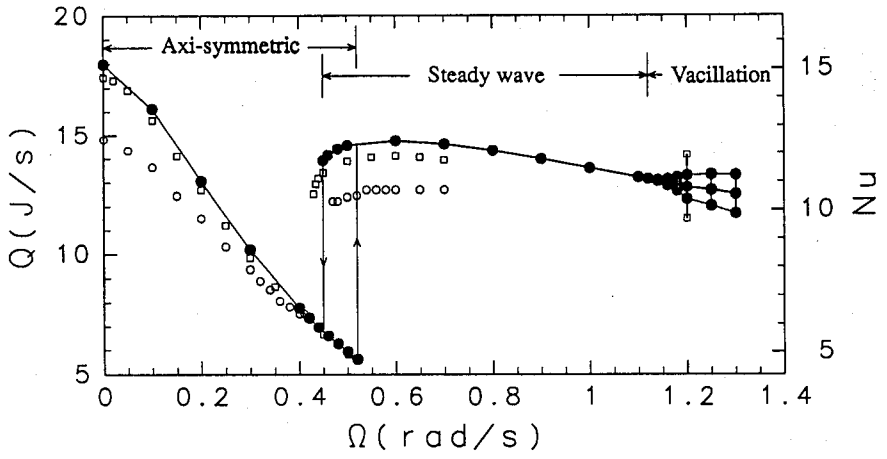

Fig. 3. Dependence of total inward heat flux Q (or, the Nusselt number Nu) on the rotation rate Ω. Symbol •—• is for the present model; ○, laboratory experiment by Ukaji and Tamaki (1989); □, numerical simulation by them. In the vacillation régime the variable range and time average are plotted. The amplitude of the vacillation obtained by Ukaji and Tamaki is overestimated because it is taken from limited plots in their figure.

$$u_r + \frac{u}{r} + \frac{v_\lambda}{r} + w_z = 0, \tag{5}$$

where (r, λ, z) are cylindrical coordinates, and t time. The corresponding velocity components are (u, v, w). Dimensionless temperature θ is defined as $\theta \equiv (T - T_a)/\Delta T$. Density is denoted by ρ, and p is pressure divided by the mean density ρ_0. The viscosity term is not the conventional form in order to avoid a round-off error in computation (Williams, 1969). Physical parameters of water are assumed to be constant at the mean temperature 26.5°C: the kinematic viscosity, $\nu = 8.65 \times 10^{-3}\,\mathrm{cm^2\,s^{-1}}$; the diffusivity of heat, $\kappa = 1.45 \times 10^{-3}\,\mathrm{cm^2\,s^{-1}}$; the coefficient of volume expansion, $\alpha = 2.71 \times 10^{-4}\,\mathrm{K^{-1}}$.

In order to get a semi-spectral form of the equations, we decompose each dependent variable into the axisymmetric part and wave parts as follows:

$$x(r, \lambda, z, t) = X(r, z, t) + \sum_{n=1}^{N} \mathrm{Re}\left[x_n(r, z, t) e^{imn\lambda}\right] \tag{6}$$

where x denotes u, v, w, θ or p. Here periodicity in the azimuthal direction is assumed with $\Delta\lambda = 2\pi/m$, and x_n (r, z, t) is the complex amplitude of a dominant wave $(n=1)$ and its higher harmonics $(n = 2, 3, \cdots)$. Substituting these expressions into (1)–(5) and making a finite difference approximation in r, z and t, we obtain a semi-spectral form of the governing equations. The same finite difference method as in Williams (1969) is adopted. The grid resolution is determined after a convergence test of the solutions; 64 (r-direction) × 64 (z-direction) and $\Delta t = 2.5 \times 10^{-2}$ s.

The assumption of the azimuthal periodicity is validated with the laboratory experiment by TU85; their careful measurement with a precise apparatus showed that the amplitudes of the side-bands and the longest wave are of the order of 1 % of the total temperature variation (~the dominant wave + its higher harmonics) not only in steady wave régime but in vacillation. Moreover, both the laboratory experiment (TU85) and the numerical experiment (UT90) showed that the amplitude of the higher harmonics decreases exponentially with n; the first harmonic is less than 20 % of the dominant wave and the second harmonic is less than 10 %. Based on this fact, we retain only a few wave components and truncate at $N=2$ for computational efficiency unless otherwise mentioned. The severe truncation in the azimuthal direction limits the application of the model to irregular turbulent flow. However, the model shows good performance in the steady wave and vacillation régimes if we compare our result with the laboratory and numerical experiments by UT89 and UT90.

A renormalization technique to keep the temperature field as $0 \leq \theta \leq 1$ is adopted following Miller and Butler (1991). If we truncate at $N=1$, the model is basically the same as theirs except for the grid resolution and spacing. A two-dimensional model developed by Sugata and Yoden (1992) is used to obtain axi-symmetric flows, and a linearized model by Sugata and Yoden (1991) is also used for the linear stability analysis of the obtained axi-symmetric flow.

Regime transitions are investigated along the line of $\Delta T = 3$ K in Fig. 1; the temperature difference is the same as that imposed by UT89 and UT90 in their laboratory experiment and numerical simulation. The semi-spectral model is integrated for 20 minutes in physical time from an initial condition

which is the flow obtained at slightly different Ω. If the obtained flow is not converged sufficiently to a steady or a vacillating state, additional time integration is done for 20 minutes more. The dominant wavenumber is fixed at $m=5$ from the observation in their laboratory experiment.

3. Results

Figure 3 shows the dependence of the flow régime on the rotation rate Ω obtained with the present semi-spectral model (dots), together with the results in laboratory experiment (open circles) and in numerical simulation (open squares) obtained by UT89. The ordinate is the inward heat flux (scale of the left side), or the Nusselt number (scale of the right side). For small Ω, only the axi-symmetric steady flow is obtained; the heat flux decreases monotonously with increasing Ω. The axi-symmetric flow becomes unstable at $\Omega=0.53$ rad/s, and a three-dimensional steady wave solution is obtained in time-integrations. The heat flux increases from 5.5 J/s to 14.8 J/s at this transition.

Branching of steady wave solutions was explored with changing the external parameter Ω. If Ω is decreases, the régime transition from the steady wave solution to axi-symmetric flow takes place at $\Omega=$ 0.45 rad/s. Therefore the present model has hysteresis between $\Omega=0.45$ rad/s and 0.53 rad/s; two stable solutions are obtained for the same external conditions depending on the initial condition. The numerical simulation by UT89 shows similar hysteresis although their laboratory experiment does not show it explicitly.

If Ω is increased, the steady wave solution becomes unstable at $\Omega=1.12$ rad/s, and vacillation solutions are obtained for higher rotation rates than that. The heat flux fluctuates purely periodically in the vacillation régime and its variable range and time mean are shown in Fig. 3. The variable range of the heat flux fluctuation increases with increasing Ω. A single numerical simulation of the vacillation at Ω $=1.2$ rad/s by UT90 has comparable fluctuation of the heat flux. (They did not show the heat flux in the laboratory experiment for this vacillation.)

The spatial structure of steady wave solutions resembles qualitatively that obtained by Williams (1971, 1972) with different experimental parameters and different grid resolutions, and resembles quantitatively that obtained by UT89 with the same experimental parameters but a different model. Only the streamfunction of the deviatoric horizontal velocity field is shown in Fig. 4 for the steady wave solution at $\Omega=0.45$ rad/s, which is very close to the critical value for the transition. The streamfunction field shows a typical pattern of baroclinic annulus waves; for example, westward tilt of the minimum (maximum) phase with height. The higher harmonic of $n=2$ is not negligible, particularly in middle and

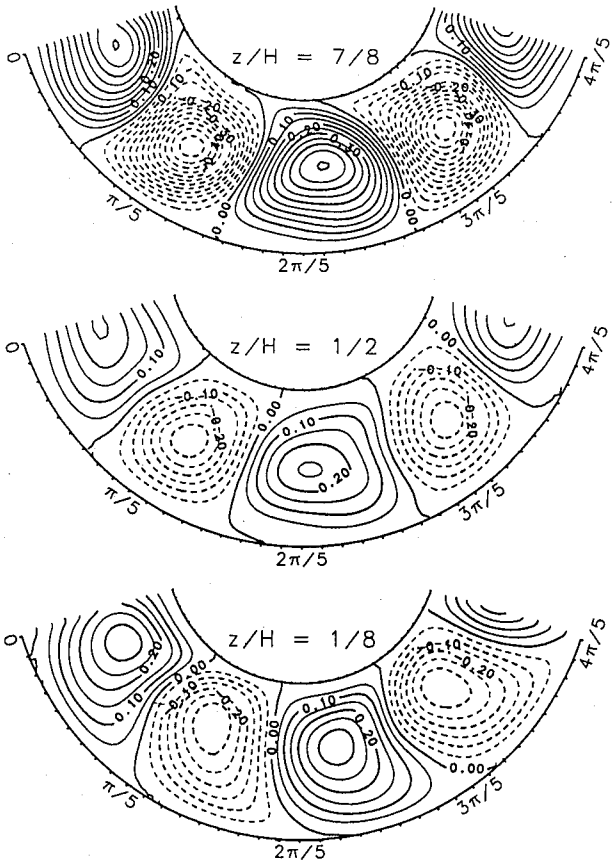

Fig. 4. The streamfunction for the deviatoric horizontal velocity field at three levels. $\Omega=0.45$ rad/s. Positive regions indicate clockwise circulation. The unit is cm^2/s.

upper layers; cyclonic circulation is more intensive than anti-cyclonic circulation and the azimuthal extent of the former is narrower. Tilts of the phase lines in a radial direction indicate non-separable nature in the instability of baroclinic axi-symmetric flow with lateral shear.

In order to investigate the flow régime transitions in the present model further, we take notice of the spatial symmetry of the flow field. The flow field is expanded in an appropriate orthogonal functions, using a Fourier-Bessel series for the present annular geometry, for comparison with Lorenz's results (1962, 1963). The radial structure of some of the lowest modes for the streamfunction is shown in Fig. 5: axisymmetric components (a), wave components for the dominant wave (b), and for the first higher harmonic (c).

Figure 6 shows the amplitude of these components for the streamfunction at the mid-depth for each Ω. The dominant wave has the same order of amplitudes as the axi-symmetric components, but the first higher harmonic is one order smaller than the dominant wave. The first radial mode in each component has the largest amplitude and other modes

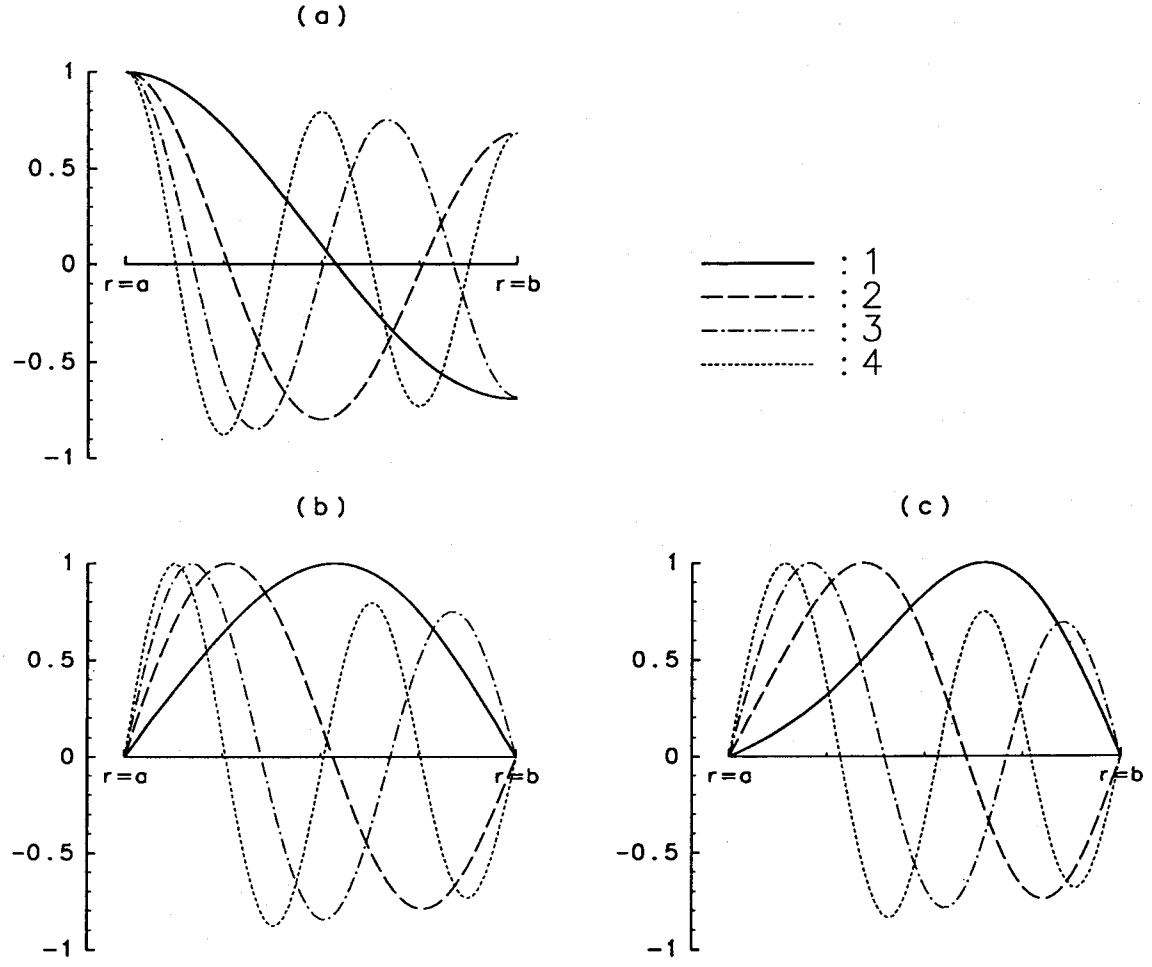

Fig. 5. Radial structure of four lowest modes of the orthogonal functions (Fourier-Bessel functions). (a) the axi-symmetric part, (b) the dominant wave of $m=5$, and (c) its first higher harmonic ($mn=10$).

have small but non-zero amplitudes. Note that all of the solutions we obtained have both odd and even radial modes, in contrast to Lorenz's (1963) result. A steady wave solution with only odd radial mode(s) (R_1 in Fig. 2) can exist as well as that with both modes (R_{12}) in the Lorenz model. Near the transition point $\Omega=0.45$ rad/s, each amplitude varies as $a\sqrt{\Omega}+b$ (a and b are constants), which dependence on Ω reminds us of the limit point of steady solutions (Matsuda, 1983). Moreover, the regime transition from steady wave to vacillation has basic characteristics of Hopf bifurcation; bifurcation of a periodic solution from a steady solution as the latter loses its stability.

The phase relation between any two modes in vacillation is well described by a trajectory projected onto a plane in phase space, which presentation was originally introduced by Lorenz (1963). Figure 7 shows the periodic trajectory of vacillations for $\Omega=1.14$–1.3 rad/s projected onto $\psi_{k0}-\psi_c$ plane where ψ_{k0} and ψ_c have similar definitions to these of Lorenz (1963): ψ_{k0} is the amplitude of the first mode of the dominant wave and ψ_c that of the second axi-symmetric mode. Clearly it is an unsymmetric vacillation (UV) in Lorenz's classification because of the asymmetry of the trajectory with respect to $\psi_c=0$. The present model does not have any correspondence to the pairing of unsymmetric vacillations with opposite sign of even modes obtained in the Lorenz model (1963) (UV' and UV'' in Fig. 2); only one unsymmetric vacillation is obtained for a given external parameter. Nearly elliptic trajectories indicate that the fluctuation of ψ_{k0} leads slightly that of ψ_c for $\Omega\leq 1.2$ rad/s, while it lags slightly for $\Omega=$ 1.25 and 1.3 rad/s.

The period of the vacillation is 50 s at $\Omega=1.14$ rad/s, and increases slightly up to 56 s at $\Omega=1.3$ rad/s. The period is a half of that obtained by UT90; their result is suggestive of a period-doubling (sub-harmonic) bifurcation of the vacillation solution with the same period of 50 s. We did not obtain any example of such a period doubling nor a non-periodic (chaotic) solution for $\Omega\leq 1.3$ rad/s.

4. Discussion

The régime transitions from steady axi-symmetric

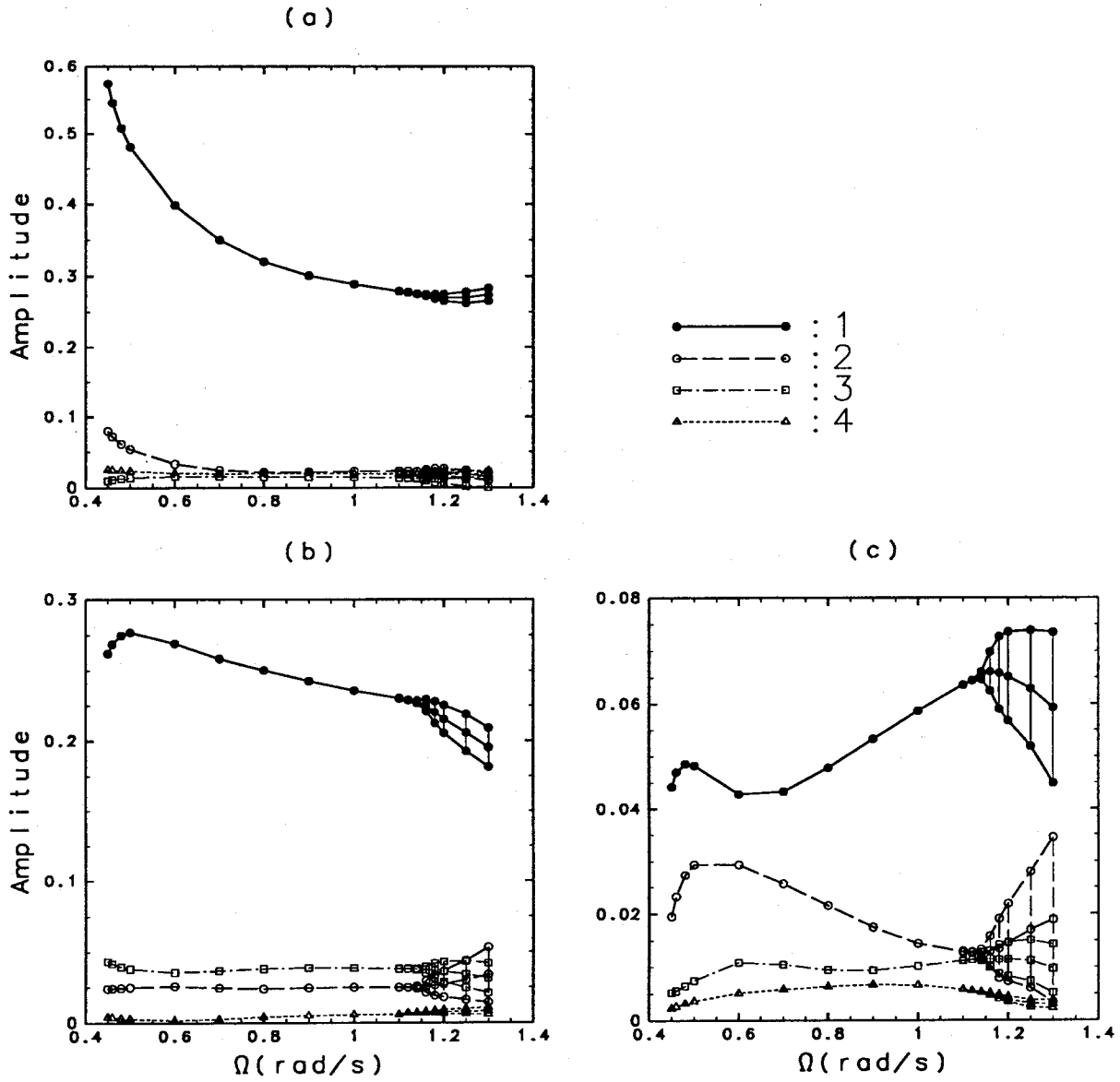

Fig. 6. The amplitude of each mode of the streamfunction for the horizontal velocity at the mid-depth. (a) the axi-symmetric part, (b) the dominant wave of $m=5$, and (c) its first higher harmonic ($mn=10$).

flow to vacillation obtained in this study are summarized in a schematic bifurcation diagram (Fig. 8). A two-dimensional axi-symmetric solution (denoted by H) is obtained for any Ω as in Sugata and Yoden (1992), but it becomes unstable at a certain value of Ω (the point A). An exponentially growing perturbation is obtained by time integrations of the linearized model with respect to the basic axi-symmetric flow. The streamfunction of the horizontal velocity of the growing perturbation near the transition point A is shown in Fig. 9. The spatial pattern of the perturbation differs qualitatively from that of the steady wave solutions (R_{12}^{m+2m}) as shown in Fig. 4, particularly in lower layers. Here, the subscript 12 of R_{12}^{m+2m} stands on both odd and even radial modes, and the superscript $m+2m$ stands on both the dominant wave and its higher harmonics. Note that the basic flow is stable for other wave perturbations except for the wavenumber 5. Non-linear time-integrations of the present model from an initial condition of the unstable basic axi-symmetric flow with the growing perturbation show attraction to the steady wave solution R_{12}^{m+2m}. No stable solution similar to the growing linear perturbation is obtained. Therefore it is concluded from the bifurcation theory (Matsuda, 1983) that this is a subcritical bifurcation of an *unstable* steady wave solution at the point A as denoted by a dashed line R_{12}^{m}.

The steady wave solution (R_{12}^{m+2m}) disappears at another transition point B, which is classified as a limit point from Figs. 3 and 6. Hysteresis is realized by the coexistence of the subcritical bifurcation

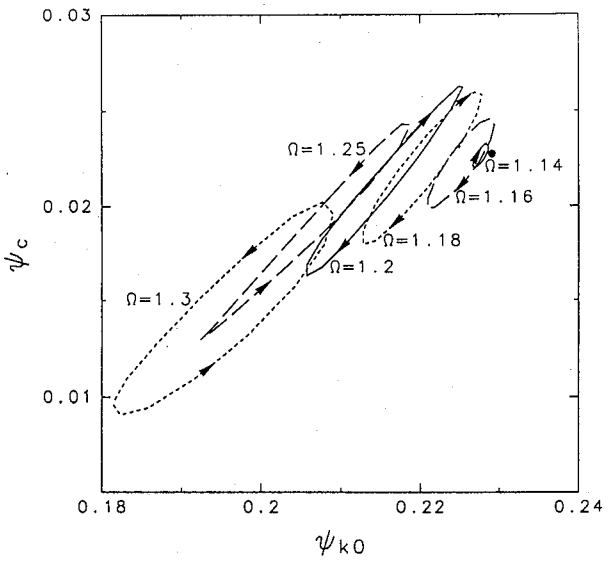

Fig. 7. Trajectories of vacillation projected onto a $\psi_{k0}-\psi_c$ plane (see text) for six rotation rates $\Omega=1.14$–1.3 rad/s. The dot indicates a stable steady wave solution near the critical point $\Omega=1.12$ rad/s.

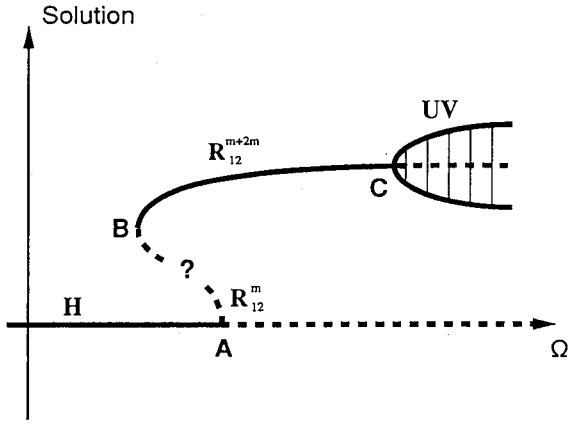

Fig. 8. Bifurcation diagram for the present result. The solid line is a branch of stable solutions, dashed line that of unstable ones. See text for details.

point A and the limit point B. The unstable branch of the steady wave from the point B may not be directly connected with the unstable branch R_{12}^m because of the existence of the higher harmonics. However, it is practically impossible to search for the unstable solutions computationally as in the Lorenz model, because the present model is a huge nonlinear system with degree of freedom of $O(10^5)$.

We did not obtain any steady wave solution which consists of only odd radial modes, in contrast to that in the Lorenz (1963) model (R_1 in Fig. 2). The reason is the difference in the symmetry group of the orthogonal functions. Lorenz (1963) assumed

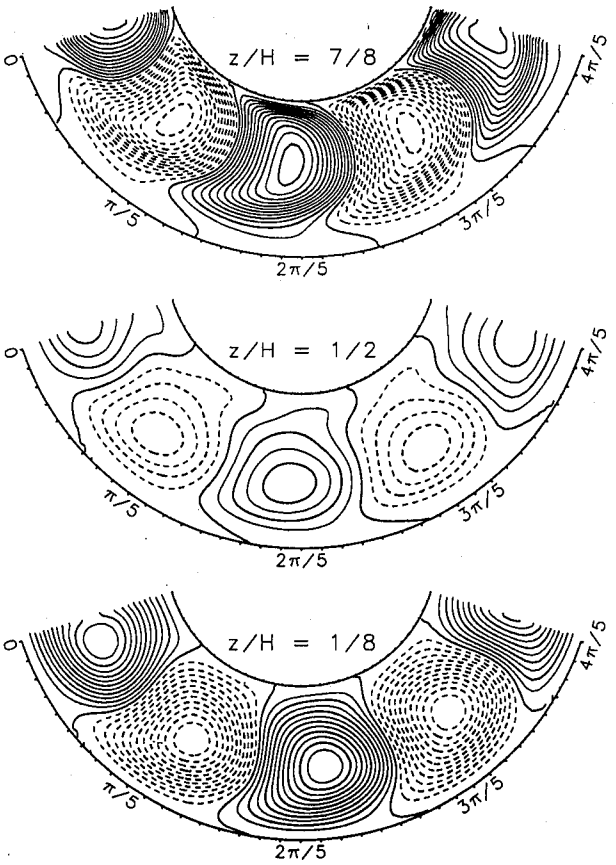

Fig. 9. As in Fig. 4, except for the most unstable wave perturbation obtained in the linear stability analysis of the axi-symmetric flow at $\Omega=0.54$ rad/s. The contour intervals are the same among the three figures.

an infinite channel to expand the field variables in a double-Fourier series, which are divided into two symmetric groups depending on the lateral structure of each mode; symmetric and anti-symmetric groups with respect to the center of the channel (see Yoden, 1985). The symmetric group constitutes a subsystem of the system, setting the anti-symmetric group to be zero. However, the present model does not have such a sub-system because of the spatial structure of the Fourier-Bessel series (Fig. 5). Therefore any steady solution in which some modes are equal to zero was not obtained. In other words, the stepwise transition from the symmetric steady wave solution (R_1) to the mixed wave solutions (R'_{12} and R''_{12}) in the Lorenz model is a spurious result due to the assumption of an infinite channel; such a transition is not possible in the annular geometry.

A vacillation solution bifurcates at the point C in Fig. 8, which is a counterpart of the point D′ (D″) in Fig. 2. The steady wave solution R_{12}^{m+2m} becomes unstable at that point indicating a Hopf bifurcation. A period-doubling bifurcation nor other transition routes to non-periodic solutions were not

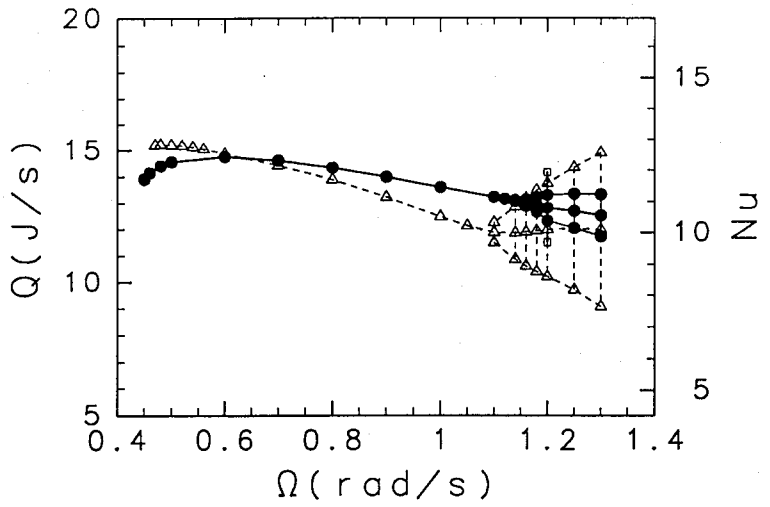

Fig. 10. As in Fig. 3, except that the symbol △---△ is for another truncation $N=1$.

obtained for $\Omega \leq 1.3$ rad/s. If the rotation rate is increased further, such transitions to an irregular régime might be obtained in the present model, even though the assumption of azimuthal periodicity may not be very appropriate.

To investigate the rôle of the first higher harmonics in the transitions of flow régimes, another model with more severe truncation of $N=1$ is used, which is basically the same as that used by Miller and Butler (1991). Figure 10 is a comparison of the inward heat flux for the two results obtained from $N=1$ (dashed line) and $N=2$ (solid line) truncations. Both of the hysteresis between the axi-symmetric and steady wave régimes and bifurcation of vacillation from the steady wave branch are obtained, even in the truncation of $N=1$. The first higher harmonic is not necessary for a qualitative understanding of the transitions from axi-symmetric flow to vacillation, although it is not negligible for quantitative arguments. The spatial structure obtained in these two models is compared with those obtained in the fully three-dimensional model and in the laboratory experiment by UT90. Figure 11 shows an azimuthal vertical cross section of the deviatoric temperature at the mean radius of the annulus for the steady wave at $\Omega=0.6$ rad/s. The $N=2$ model (a) gives a very similar result as the full model (c) and the laboratory experiment (d). However, the $N=1$ model (b) with no higher harmonics has some differences, particularly in the upper layers.

Similar numerical studies were done along the line of $\Delta T=8$ K in Fig. 1, and qualitatively similar results to those for $\Delta T=3$ K were obtained. Any amplitude vacillation adjacent to a transition to the steady axi-symmetric flow, which is observed in the laboratory experiments (Fig. 1), is not obtained in the present model. It is conjectured from bifurcation theories that the sudden disappearance of the vacillation comes from a limit point of a pair of periodic solution (vacillation) branches (see Fig. 1 in Yoden, 1987), but a more sophisticated model is necessary to obtain such a régime transition.

5. Conclusion

Stepwise transitions in flow régimes observed in some of the rotating annulus experiments with radial differential heating were investigated numerically with a semi-spectral model of a three-dimensional Navier-Stokes equation with a Boussinesq approximation, and the results were interpreted with bifurcation theories. Experimental conditions are identical to the laboratory experiments by Tamaki and Ukaji (1985) and Ukaji and Tamaki (1989, 1990). The rotation rate Ω is changed as a bifurcation parameter with other conditions fixed. A schematic bifurcation diagram shown in Fig. 8 is obtained as a summary of our results. Steady, two-dimensional axi-symmetric flow (denoted by H) exists for any Ω, but it becomes unstable at a critical value of Ω (the point A) with respect to a wave perturbation. However, this is a sub-critical bifurcation because no stable steady wave solution similar to the linear growing-mode is obtained near the bifurcation point. Instead, a finite-amplitude steady wave solution (R_{12}^{m+2m}) is obtained in time-integrations at the bifurcation point, the spatial structure of which is different from the linear mode. The steady wave solution disappears at another critical point B at a smaller Ω than the bifurcation point. That is, hysteresis exists between these two critical points; the sub-critical bifurcation point (A) and the limit point (B). As Ω is increased, the steady wave solution becomes unstable at the point C in Fig. 8 with respect to a perturbation which fluctuates purely periodically. Periodic solutions well known as a tilted-trough vacillation are obtained for larger Ω than this

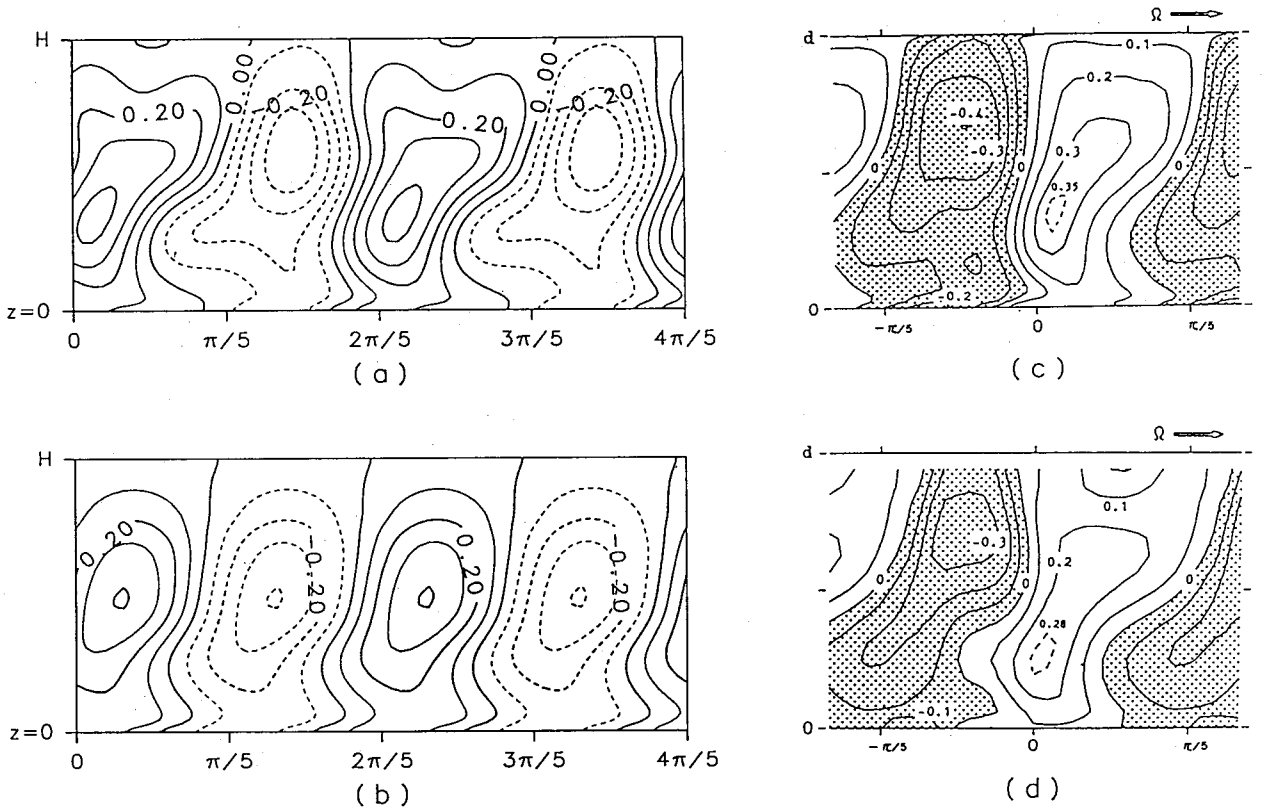

Fig. 11. Azimuthal-vertical cross sections of deviatoric temperature at the mid-radius for $\Omega=0.6$ rad/s: (a) the present model of $N=2$, (b) that of $N=1$, (c) the numerical model by Ukaji and Tamaki (1989), and (d) the laboratory experiment by them. The unit is K.

critical value. This is interpreted as a Hopf bifurcation from the trajectories shown in Fig. 7.

Contrary to the Lorenz (1963) model of a low-order system, bifurcation in the steady wave branch is not obtained in the present model. The spurious bifurcation in the Lorenz model (the point B in Fig. 2) arises from the spatial symmetry of the flow domain. In the geometry of an infinite channel assumed by Lorenz (1963), a group of symmetric components with respect to the mid-channel constitutes a sub-system of the low-order system, and a symmetry-breaking bifurcation takes place with respect to anti-symmetric components. However, such a sub-system does not exist for the present annular geometry, because of the characteristics of the Fourier-Bessel series (Fig. 5) which is the appropriate orthogonal function for this geometry.

Analysis of transitions from vacillation to the irregular régime remains as our future study, for which a full three-dimensional numerical model is necessary.

Acknowledgments

The authors wish to thank Professor I. Hirota for his valuable comments during the work. This study was partly supported by the Grant-in-Aid for Scientific Research, the Ministry of Education, Science, and Culture of Japan. The GFD-DENNOU Library was used for drawing the figures.

References

Fein, J.S., 1973: An experimental study of the effects of the upper boundary condition on the thermal convection in a rotating, differentially heated cylindrical annulus of water. *Geophys. Fluid Dyn.*, **5**, 213–248.

Fowlis, W.W. and R. Hide, 1965: Thermal convection in a rotating annulus of liquid: effect of viscosity on the transition between axisymmetric and non-axisymmetric flow regimes. *J. Atmos. Sci.*, **22**, 541–558.

Fultz, D., R.R. Long, G.V. Owens, W. Bohan, R. Kaylor and J. Weil, 1959: Studies of thermal convection in a rotating cylinder with some implications for large-scale atmospheric motions. *Meteor. Monographs*, **4-21**, 104 pp.

Ghil, M. and S. Childress, 1987: *Atmospheric dynamics, dynamo theory, and climate dynamics.* Springer-Verlag, 73–124.

Hide, R. and P.J. Mason, 1975: Sloping convection in a rotating fluid, *J. Adv. Phys.*, **24**, 47–100.

Hignett, P., 1985: Characteristics of amplitude vacillation in a differentially heated rotating fluid annulus. *Geophys. Astrophys. Fluid Dyn.*, **31**, 247–281.

Hignett, P., A.A. White, R.D. Carter, W.D.N. Jackson and R.M. Small, 1985: A comparison of laboratory measurements and numerical simulations of

baroclinic wave flows in a rotating cylindrical annulus. *Quart. J. Met. Soc.*, **111**, 131–154.

Lorenz, E.N., 1962: Simplified dynamic equations applied to the rotating-basin experiments. *J. Atmos. Sci.*, **19**, 39–51.

Lorenz, E.N., 1963: The mechanics of vacillation. *J. Atmos. Sci.*, **20**, 448–464.

Matsuda, Y., 1983: Classification of critical points and symmetry-breaking in fluid phenomena and its application to dynamic meteorology. *J. Meteor. Soc. Japan*, **61**, 771–788.

Matsuda, Y. and S. Yoden, 1985: Meteorology and catastrophe—Multiple equilibria in dynamic meteorology (in Japanese). Note on Meteorological Research, **151**, 145 pp.

Miller, T.L. and K.A. Butler, 1991: Hysteresis and the transition between axisymmetric flow and wave flow in the baroclinic annulus. *J. Atmos. Sci.*, **48**, 811–823.

Pfeffer, R.L., G. Buzyna and R. Kung, 1980: Time-dependent modes of behavior of thermally driven rotating fluids. *J. Atmos. Sci.*, **37**, 2129–2149.

Quinet, A., 1973a: The structure of non-linear processes. *Tellus*, **25**, 536–544.

Quinet, A., 1973b: Non-linear mechanisms in a non-conservative quasi-geostrophic flow which possesses 30 degrees of freedom. *Tellus*, **25**, 545–559.

Sugata, S. and S. Yoden, 1991: The effects of centrifugal force on the stability of axisymmetric viscous flow in a rotating annulus. *J. Fluid Mech.*, **229**, 471–482.

Sugata, S. and S. Yoden, 1992: Steady axi-symmetric flow due to differential heating in a rotating annulus and its dependence on experimental parameters. *J. Meteor. Soc. Japan*, **70**, 1005–1017.

Swinney, H.L. and J.P. Gollub (eds.), 1981: *Hydrodynamic instabilities and the transition to turbulence.* Springer-Verlag, 292 pp.

Tamaki, K. and K. Ukaji, 1985: Radial heat transport and azimuthally averaged temperature fields in a differentially heated rotating fluid annulus undergoing amplitude vacillation. *J. Meteor. Soc. Japan*, **63**, 168–179.

Ukaji, K. and K. Tamaki, 1989: A comparison of laboratory experiments and numerical simulations of steady baroclinic waves produced in a differentially heated rotating fluid annulus. *J. Meteor. Soc. Japan*, **67**, 359–374.

Ukaji, K. and K. Tamaki, 1990: A numerical study of tilted-trough vacillation observed in a differentially heated rotating fluid annulus. *J. Meteor. Soc. Japan*, **68**, 447–460.

Williams, G.P., 1967a: Thermal convection in a rotating fluid annulus: part 1. The basic axisymmetric flow. *J. Atmos. Sci.*, **24**, 144–161.

Williams, G.P., 1967b: Thermal convection in a rotating fluid annulus: part 2. Classes of axisymmetric flow. *J. Atmos. Sci.*, **24**, 162–174.

Williams, G.P., 1969: Numerical integration of the three-dimensional Navier-Stokes equations for incompressible flow. *J. Fluid Mech.*, **37**, 727–750.

Williams, G.P., 1971: Baroclinic annulus waves. *J. Fluid Mech.*, **49**, 417–449.

Williams, G.P., 1972: The field distributions and balances in a baroclinic annulus wave. *Mon. Wea. Rev.*, **100**, 29–41.

Yoden, S., 1979: Some dynamical properties of nonlinear baroclinic waves in a quasi-geostrophic model. *J. Meteor. Soc. Japan*, **57**, 493–504.

Yoden, S., 1985: Multiple stable states of quasi-geostrophic barotropic flow over sinusoidal topography. *J. Meteor. Soc. Japan*, **63**, 1031–1045.

Yoden, S., 1987: Bifurcation properties of a stratospheric vacillation model. *J. Atmos. Sci.*, **44**, 1723–1733.

セミスペクトルモデルを用いた回転水槽中の流れパターンの遷移に関する数値的研究

菅田誠治[1]・余田成男

(京都大学理学部)

いくつかの回転水槽実験で得られた軸対称流—定常波動—バシレーションという段階的な流れパターンの遷移を、3次元ブシネスク流体のセミスペクトルモデルを用いて調べ、分岐理論をもとに考察した。軸対称流—定常波動間の遷移は、ヒステリシスによって特徴づけられる。すなわち、得られた定常波動は、軸対称流が不安定化するところで、そこから分岐するのではなく、別の臨界点（極限点）が存在し、そこで定常波動解が消滅する。また定常波動—ティルティッド・トラフ・バシレーション間の遷移は、定常波動が不安定化するところでのHopf分岐（周期解の定常解からの分岐）によると考えられる。

[1]現在所属：国立環境研究所